Cell, Vol. 111, 77–89, October 4, 2002, Copyright ©2002 by Cell Press

Asymmetries in H^+/K^+-ATPase and Cell Membrane Potentials Comprise a Very Early Step in Left-Right Patterning

Michael Levin,[1,2] Thorleif Thorlin,[3,4] Kenneth R. Robinson,[4] Taisaku Nogi,[2] and Mark Mercola[1,5,6]

[1]Department of Cell Biology
Harvard Medical School
240 Longwood Avenue
Boston, Massachusetts 02115
[2]Cytokine Biology Department
The Forsyth Institute
140 The Fenway
Boston, Massachusetts 02115
[3]Sahlgrens University Hospital
Institute for Clinical Neuroscience
Bla Straket 7
SE 413 45 Gothenburg
Sweden
[4]Department of Biological Sciences
Purdue University
West Lafayette, Indiana 47907

Summary

A pharmacological screen identified the H^+ and K^+ ATPase transporter as obligatory for normal orientation of the left-right body axis in *Xenopus*. Maternal H^+/K^+-ATPase mRNA is symmetrically expressed in the 1-cell *Xenopus* embryo but becomes localized during the first two cell divisions, demonstrating that asymmetry is generated within two hours postfertilization. Although H^+/K^+-ATPase subunit mRNAs are symmetrically localized in chick embryos, an endogenous H^+/K^+-ATPase-dependent difference in membrane voltage potential exists between the left and right sides of the primitive streak. In both species, pharmacologic or genetic perturbation of endogenous H^+/K^+-ATPase randomized the sided pattern of asymmetrically expressed genes and induced organ heterotaxia. Thus, LR asymmetry determination depends on a very early differential ion flux created by H^+/K^+-ATPase activity.

Introduction

The vertebrate body plan is outwardly bilaterally symmetric yet has consistent asymmetries in the position and anatomy of the visceral organs and brain. Much progress has been made recently in unraveling the molecular mechanisms involved in the generation of left-right (LR) asymmetries during embryonic development (Burdine and Schier, 2000; Capdevila et al., 2000; Mercola and Levin, 2001; Yost, 2001). The best understood aspect of LR asymmetry determination is the genetic cascade that transduces an initial asymmetry into cues interpretable by the developing visceral organs. Mechanisms that act upstream of asymmetric gene expression, however, remain poorly characterized. Thus, our work has focused on pursuing the determining mechanisms backward from the point of asymmetric gene expression.

Several mechanisms have been proposed to act upstream of sided gene expression to orient LR asymmetry. One model is based on the observation that the vortical movement of individual monocilia that protrude from the ventral surface of cells in the mouse node propel the leftward movement of an unknown determinant (Nonaka et al., 1998). This model is attractive because it provides a means of generating body axis asymmetry from a molecular level chirality and is consistent with the involvement of dynein and kinesin proteins associated with monocilia (Supp et al., 1999, 1997; Takeda et al., 2000, 1999). However, the difficulty in reconciling this model with experiments showing asymmetric expression of genes and patterning prior to node formation in the chick (Levin and Mercola, 1999; Pagan-Westphal and Tabin, 1998; Psychoyos and Stern, 1996; Yuan and Schoenwolf, 1998) has prompted speculation that profound differences exist between the asymmetry determining mechanisms used across vertebrate species and/or that multiple, possibly reinforcing, mechanisms operate (Capdevila et al., 2000; Mercola and Levin, 2001). *Xenopus* embryos have been widely used to probe early patterning steps and several lines of experimentation suggest that components of the LR determination mechanism act prior to the formation of Spemann's Organizer, which has signaling functions in common with the amniote node (for instance, see Hyatt and Yost, 1998; Lohr et al., 1997). In previous studies, we have shown that intercellular communication via gap junctions is an essential component of LR patterning upstream of early asymmetric gene expression in both chick and *Xenopus* embryos (Levin and Mercola, 1998, 1999). Importantly, genetic or pharmacologic disruption of gap junctional communication randomizes normally asymmetric organ anatomy and gene expression. Although clearly required for LR asymmetry, the endogenous pattern of open junctional channels would seem insufficient to orient the LR axis without a mechanism to rectify the direction of propagation of determinants through the gap junctions.

Here, we report the results of a pharmacologic screen indicating that the H^+/K^+ ATPase transporter is essential for normal LR asymmetry in developing *Xenopus* and chicks. Although endogenous ion gradients and voltages have been implicated in a number of embryonic processes (Altizer et al., 2001; Borgens and Shi, 1995; Hotary and Robinson, 1992, 1994; Jaffe, 1981; Shi and Borgens, 1994, 1995), our results identify a hydrogen/potassium flux as a very early step in LR asymmetry determination in chick and *Xenopus* embryos. We suggest that asymmetrically localized ion flux controls asymmetric gene expression, possibly by directing the propagation low molecular weight determinants through gap junction channels.

[5]Correspondence: mmercola@burnham.org
[6]Present address: The Burnham Institute, 10901 North Torrey Pines Road, La Jolla, California 92037.

Results

A Pharmacological Screen Implicates H^+ and K^+ Ion Flux in LR Asymmetry

In order to determine whether endogenous ion flux is important for LR patterning during development, we took advantage of the ease of exposing large numbers of *Xenopus* embryos to compounds in medium, as well as the plethora of available pharmacological agents that target various ion channels and pumps. Drugs of increasing specificity were used in successive reiterations of the screen in order to narrow down the lead candidate proteins. In preliminary studies, we determined the levels of each drug that did not cause general developmental defects in *Xenopus*. Surprisingly, embryos readily tolerated high concentrations of a number of ion channel and pump blockers. In each experiment, eggs from individual females were divided into groups of about 100 embryos each. The internal control group was cultured in 0.1×MMR containing the same amount of vehicle as the experimental groups. Experimental groups were cultured in 0.1×MMR containing levels (see Experimental Procedures) of each compound that were titered to sufficiently low concentrations to permit absolutely normal embryonic development and morphogenesis of the heart and gut other than situs anomalies. The normal dorsoanterior development (dorsoanterior index, DAI, of 5) and normally spaced eyes of the treated embryos indicate that the effects on LR asymmetry described below are not the consequence of compromised dorsoanterior patterning. Embryos were allowed to develop in solution until stage 16, at which point they were washed extensively and cultured in 0.1×MMR until stage 45. At that stage, anesthetized tadpoles were scored visually for the situs of the heart, gut coiling, and gallbladder. A defect in the laterality of any of those three organs was scored as an instance of heterotaxia.

Figure 1A summarizes a sample of the data resulting from the pharmacological screen. The maximum level of heterotaxia theoretically possible from the randomization of three organs is 87.5% if each occurs independently. Lower incidences are generally observed because situs of an individual organ can be influenced by that of adjacent organs [e.g., disturbances in gut rotation correlate with an inversion of gallbladder situs (Casey, 1998)] and the drug doses, which were chosen to preclude defects that might secondarily affect situs (such as effects on dorsoanterior patterning), are likely to be suboptimal for perturbing laterality. Untreated control embryos exhibit approximately 1% incidence of heterotaxia. Numerous compounds were found to have no specific effect on LR asymmetry, including spermine, p-chloromercuribenzenesulphonate (PCMB), amantadine, indanyloxyacetic acid (IAA), 5-nitro-2-(3-phenylpropylamino)benzoic acid (NPPB, PAA), tetrodotoxin, veratridine, quinidine, lanthanum, and amiodarone. The pharmacological profile of the compounds that do not affect organ laterality argues against the involvement of a broad range of targets (assuming no permeability barriers), including aquaporins, calcium, sodium, chloride, and ligand-gated NMDA channels.

In contrast, $BaCl_2$ and the KvLQT-1 channel blocker chromanol 293B (Jiang and MacKinnon, 2000) caused 32% and 45% incidences of heterotaxia, respectively, in the absence of other defects (Figure 1A and Supplemental Table S1 available at http://www.cell.com/cgi/content/full/111/1/77/DC1). As these affect potassium flux, we then examined lansoprazole, a blocker of the H^+/ K^+-ATPase pump (Sanders et al., 1992) and found that it induced heterotaxia in 51% of the embryos.

Inhibitors of H^+/K^+-ATPase Activity Cause Heterotaxia

The H^+/K^+-ATPase is a well-studied heterodimer consisting of a larger α subunit responsible for transport and catalytic functions and a smaller glycosylated β subunit with structural and membrane-targeting functions (Gottardi and Caplan, 1993a, 1993b; Sachs et al., 1995). In a number of epithelial cells, including gastric parietal cells, H^+/K^+-ATPase in the apical plasma membrane pumps H^+ out of the cell in exchange for K^+ at the expense of ATP hydrolysis. Three specific inhibitors confirm that LR defects are caused by disruption of H^+/K^+-ATPase function (Figure 1B). *Xenopus* embryos exposed between stages 1 and 16 to omeprazole (Mizunashi et al., 1993), SCH28080 (Munson et al., 2000), and lansoprazole (Sanders et al., 1992) exhibited 30%, 42%, and 51% incidences of heterotaxia, respectively. In contrast, Na^+/H^+ exchanger blockers such as amiloride (Harris and Fliegel, 1999), ethylisopropylamiloride (EIPA; Pizzonia et al., 1996), and cariporide (Mathur and Karmazyn, 1997) had only a very modest or no effect (6%, 4%, and 1% incidences of heterotaxia, respectively). Likewise, treatment with the Na^+/K^+-ATPase inhibitor ouabain (Croyle et al., 1997) or the mitochondrial F-ATPase inhibitor aurovertin (Weber and Senior, 1998) induced only 8% and 1% incidences, respectively. Thus, the pharmacological profile strongly implicates H^+/K^+-ATPase activity in LR axis orientation.

Visceral organs of treated *Xenopus* embryos developed asymmetrically, but with either normal or LR reversed anatomy (Figures 1C–1G). Note that the heads of treated embryos developed normally, with widely spaced eyes. Head and eye anatomy are sensitive indicators of early dorsoanterior patterning; thus, the conditions of the assay did not alter dorsoanterior pattern. Although LR reversal of the viscera (situs inversus) was observed frequently, individual reversals of the heart, as well as reversal of gut and gallbladder together were also common (Supplemental Table S1 available at above website) and similar for the three drugs. Thus, disruption of H^+/K^+-ATPase activity resulted in heterotaxia (discordant asymmetry of visceral organs), rather than situs inversus or isomerism (loss of asymmetry). Similarly, chick embryos treated by injection of lansoprazole, omeprazole, or SCH28080 into the albumin prior to incubation and maintained in ovo until HH stage 15 had frequent heart reversals but were otherwise anatomically correct [Figures 1H and 1I; 0% of untreated embryos ($n = 62$) and 14% of injected embryos ($n = 28$) exhibited reversals indicating a significant effect, $p < 0.01$ from chi-square analysis].

Inhibitors of H^+/K^+-ATPase Affect an Early Developmental Process and Disrupt Normal Asymmetric Gene Expression

The current understanding of LR determination is that an early biasing mechanism orients the LR axis and

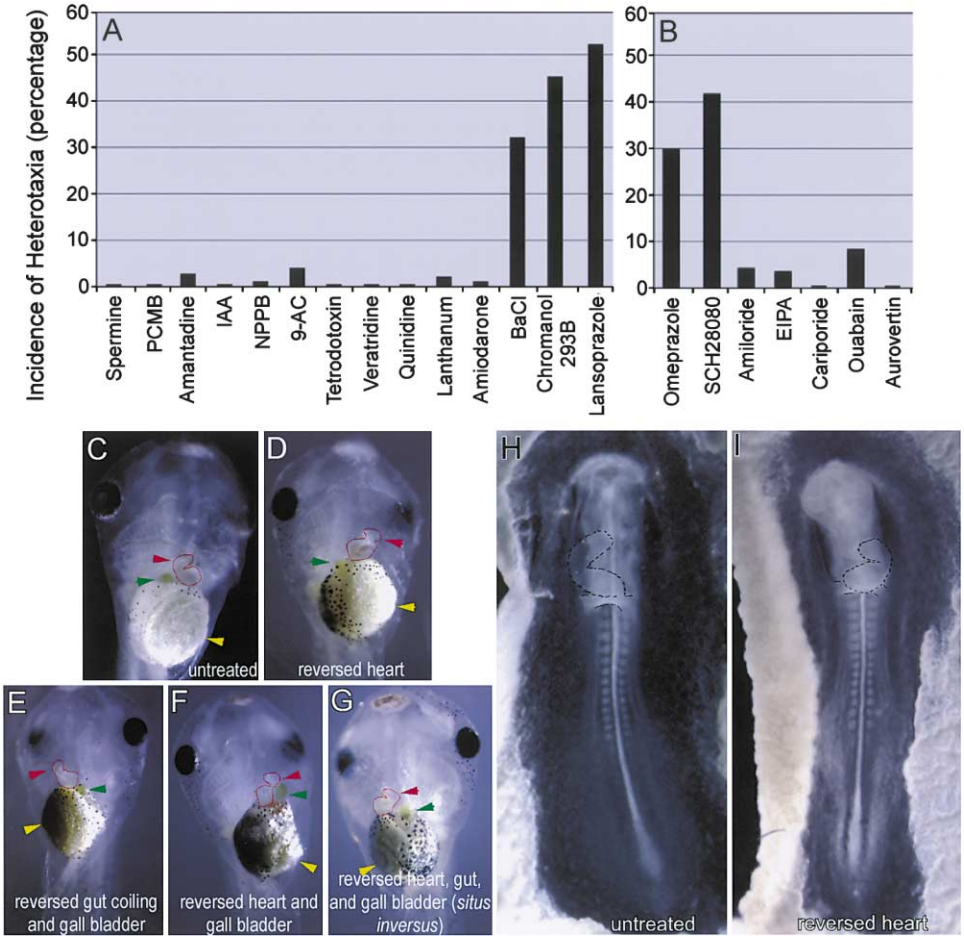

Figure 1. Pharmacological Screen Implicates K^+ and H^+ Ion Flux in LR Patterning

(A) K^+ channel ($BaCl_2$ and Chromanol 293B) and H^+ pump (lansoprazole) inhibitors induced high incidences of heterotaxia. Batches of *Xenopus* embryos were exposed to ion channel and pump inhibitors between fertilization and stage 16 and scored for the laterality of the heart, stomach coiling, and gallbladder at stage 45. The incidence of heterotaxia in control embryos was about 1%.

(B) H^+/K^+-ATPase blockers (omeprazole and SCH28080) induced heterotaxia whereas amiloride, EIPA, and cariporide (which inhibit Na^+/H^+ exchangers), ouabain (which inhibits Na^+/K^+-ATPase), and aurovertin (which inhibits the mitochondrial H^+-ATPase) did not cause significant incidences of heterotaxia at doses that do not elicit anterioposterior defects.

(C–G) Analysis of the situs of the heart, gut coiling, and gallbladder position of *Xenopus* embryos exposed H^+/K^+-ATPase inhibitors. Ventral views of stage 45 embryos are shown. Red arrowheads indicate the apex of the heart, yellow arrowheads indicate the direction of gut coiling, and green arrowheads indicate the gallbladder.

(H and I) Example of normal heart in untreated and reversed heart in chick embryos injected in the albumin with lansoprazole and cultured in ovo to stage 15. Identical results were obtained with omeprazole and SCH28080.

that this information is conveyed, through a cascade of asymmetric gene expression, to the organ primordia. The developing primordia rely on the LR cues to dictate the direction of asymmetric morphogenesis, but not asymmetric morphogenesis per se. Accordingly, failure to initiate or propagate the early biasing signal (such as is envisaged in *Kif3b*$^{-/-}$ or *iv/iv* mice) randomizes the normal sided expression of asymmetric genes and causes organs to develop either normal or inverted situs, with roughly comparable incidences. Thus, H^+/K^+-ATPase inhibitors might perturb the early biasing mechanism or uncouple it from downstream events. Consistent with this model, exposure to $BaCl_2$ or lansoprazole from fertilization to stage 8 (mid-blastula transition, MBT), when zygotic transcription ensues, induced heterotaxia [25% ($n = 80$) for $BaCl_2$, 42% ($n = 92$) for lansoprazole]. In contrast, exposure from stages 8–12 or from stage 12 onward did not induce significant incidences of heterotaxia [stages 8–12, 3% heterotaxia, ($n = 92$) for lansoprazole; stage 12 onward, $< 3\%$ ($n = 101$) for $BaCl_2$, $< 5\%$ ($n = 62$) for lansoprazole]. As would be predicted for an early component of asymmetry determination, inhibition of H^+/K^+-ATPase function altered asymmetric gene expression. Exposure to lansoprazole caused bilateral or right-sided *XNr-1*, *Pitx-2*, and *lefty* at the expense of normal left-sided expression (Figure 2, Supplemental Table S2A available at above website). Identical results were obtained with omeprazole and SCH28080 (not shown).

We next examined genes involved in LR asymmetry in the chick. In addition to generalizing the *Xenopus* results to another vertebrate species, the hierarchy of

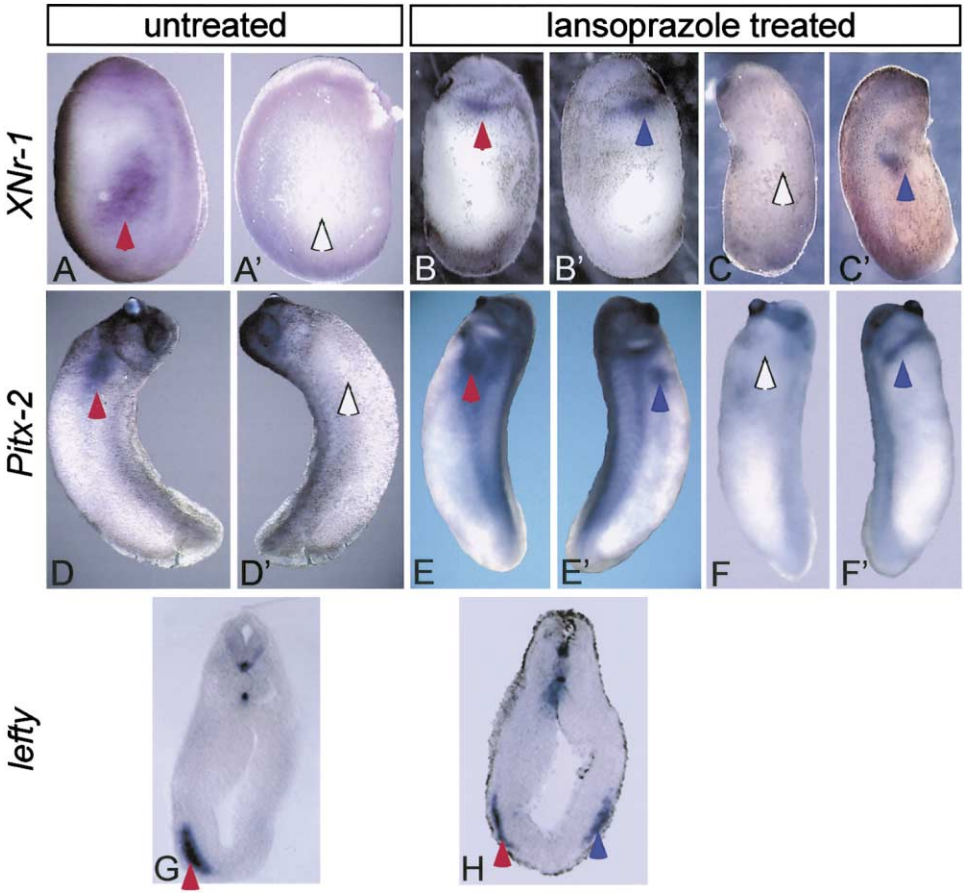

Figure 2. Inhibitors of H^+/K^+-ATPase Activity Perturb Sidedness of Asymmetric Gene Expression in *Xenopus*

Examples of ectopic right-sided and absent expression of genes normally expressed in the left lateral mesoderm as detected by in situ hybridization.

Left (A–F) and right (A′–F′) flanks of embryos probed for *XNr-1* (A-C′, stages 22–24), *Pitx-2* (D–F′, stages 28–30) expression.

(G and H) Transverse histological sections of stages 28–30 embryos showing left-sided *lefty* expression in an untreated embryo (G) and bilateral expression in a treated embryo (H). In all images, arrowheads indicate normal (red), absent (white) or ectopic (blue) expression.

asymmetrically expressed genes is more completely characterized in the developing chick. Embryos maintained either in filter culture or in ovo and exposed to lansoprazole, omeprazole, or SCH28080 frequently exhibited bilateral or absent expression of *Shh* at the edge of Hensen's node, where expression is normally left-sided at HH stage 5 (Figures 3A and 3B; Supplemental Table S2B available at http://www.cell.com/cgi/content/full/111/1/77/DC1). *Wnt8-C* and *fgf8* are normally expressed on the right side of Hensen's node at HH stage 5 and exposure caused frequent absent or bilateral expression (Figures 3C–3G; Supplemental Table S2B available at above website). Similarly, H^+/K^+-ATPase inhibitors unbiased the normally left-sided expression of *Nodal* and *Pitx-2* in the lateral plate mesoderm (LPM) (Figures 3H–3K; Supplemental Table S2B available at above website). Interestingly, for *Wnt8C*, the incidence of embryos with absent exceeded that with bilateral expression, but for *Shh* and *fgf8*, bilateral expression predominated in affected embryos. In addition, the incidence of absent or bilateral expression exceeded unilateral right-sided expression of genes normally transcribed on the left in the chick, whereas unilateral right-sided expression of *XNr-1* and *Pitx-2* was observed more frequently in *Xenopus* (compare Supplemental Tables S2A and S2B available at above website). These species and gene differences are interesting but not yet understood. Nonetheless, we conclude that H^+/K^+-ATPase activity is required in both species for correct LR patterning of asymmetric gene expression.

Head Laterality Is also Affected by H^+/K^+-ATPase Inhibitors

Laterality in the head is characterized by consistent direction of head turning in amniotes and extends to neurological asymmetries such as involved in language processing in humans. Whether any aspect of head asymmetry is determined by the mechanisms that pattern visceral organ asymmetry is controversial. It has been proposed, for instance, that head turning is influenced by the direction of heart looping (Waddington, 1937) and, by extension, the *Shh-Nodal-Pitx-2* pathway. We have previously shown, however, that *caronte/cCerberus* (referred to here as *car*) is asymmetrically expressed in the left LPM and head mesenchyme but that it is regulated by Nodal only in the head and not in

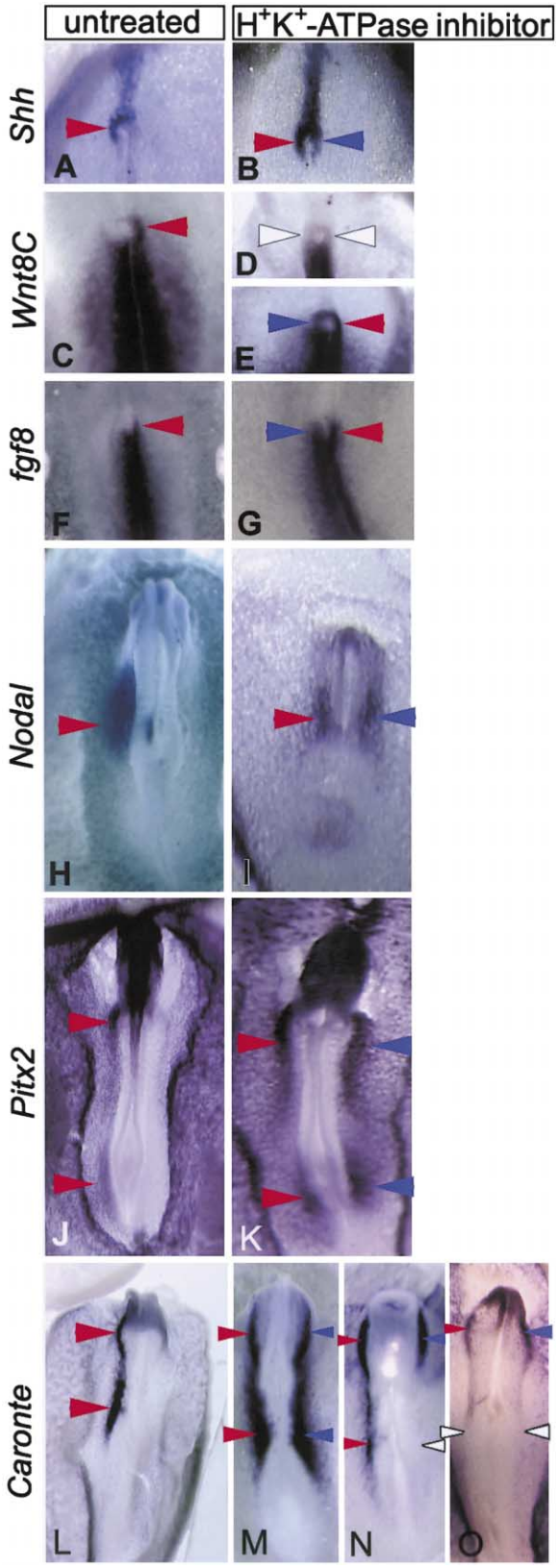

Figure 3. Aberrant Expression of Normally Asymmetrically Expressed Genes in Chick Embryos Treated with H^+/K^+-ATPase Inhibitors
Identical results were obtained with SCH28080, lansoprazole, and omeprazole and typical examples are shown here.

the LPM (Zhu et al., 1999). As *car* is the only known genetic marker of head polarity in the chick, we used it to ask whether H^+/K^+-ATPase function affects both the head and LPM domains or acts primarily on one of these systems. Interestingly, treatment of chick embryos with H^+/K^+-ATPase inhibitors randomized the expression of both LPM and head expression of *car* independently (Supplemental Table S2C available at above website), resulting in instances of bilateral expression in both the flank and head (Figure 3M), ectopic right-sided head expression (Figure 3N), and ectopic right-sided expression in the head combined with a lack of the endogenous left-sided flank expression (Figure 3O). The effects on *car* indicate that inhibiting H^+/K^+-ATPase function might uncouple at least some aspects of head and visceral organ asymmetry.

H^+/K^+-ATPase Subunit mRNA Becomes Asymmetrically Localized Shortly after Fertilization

In the unfertilized *Xenopus* egg, H^+/K^+-ATPase α mRNA is present in a radially symmetrical, circular region at the animal pole (Figure 4A). By the 4-cell stage, the mRNA has become selectively depleted in the left ventral blastomere (Figure 4C, white arrowhead). Histological sections through the animal hemisphere of 4-cell embryos show that the mRNA is localized selectively to subcortical region of both dorsal and right ventral blastomeres, but is only faintly visible in the left ventral blastomere (Figures 4D–4F). Asymmetric localization of H^+/K^+-ATPase α mRNA occurs during the first two cell cycles and is visible in about a third of the embryos after the first cleavage (Figure 4B). LR asymmetric localization of mRNA prior to zygotic transcription is unprecedented to our knowledge and, importantly, constrains the initial determination of asymmetry to within the first few hours following fertilization (see Discussion). Expression in the dorsal blastomeres remains symmetric. At the 8-cell stage, H^+/K^+-ATPase α mRNA is visible in dorsal animal blastomeres and the animal-most part of dorsal vegetal blastomeres (Figure 4G). After the onset of embryonic transcription at MBT (stage 8), expression becomes symmetrical and is localized to the animal cap (Figure 4H). H^+/K^+-ATPase α mRNA continues to be expressed in tailbud stages, primarily in the head and posterior gut (Figure 4I). Thus, the early asymmetric localization of H^+/K^+-ATPase mRNA coincides with sensitivity to the inhibitors and, to our knowledge, is the earliest known LR asymmetry in vertebrates.

(A–G) HH stage 5 embryos probed for *Shh*, *Wnt8C*, and *fgf8* expression by in situ hybridization. Treated embryos show bilateral or absent perinodal expression (B, D, E, and G).
(H and I) *Nodal* expression in HH stage 8 embryos.
(J and K) *Pitx-2* expression seen at HH stage 11.
(L–O) Left flank and head mesenchyme expression of *Caronte* at HH stage 9 (L, red arrowheads). Examples of aberrant expression of both domains in embryos exposed to H^+/K^+-ATPase inhibitors include bilateral head and flank (M), head but not flank (N), and absent flank with bilateral head (O) expression. In all images, arrowheads indicate normal (red), absent (white), and ectopic (blue) expression.

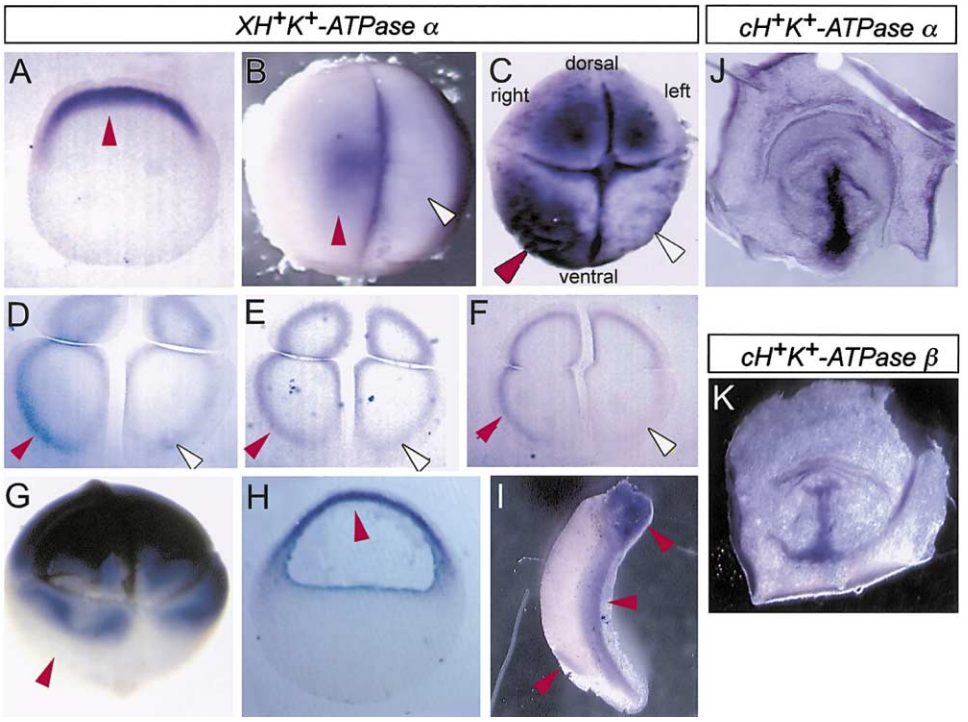

Figure 4. H^+/K^+-ATPase mRNA in *Xenopus* and Chick Embryos

(A) H^+/K^+-ATPase α mRNA is localized preferentially to the animal hemisphere of the unfertilized *Xenopus* egg (shown in histological section).
(B and C) Animal views showing asymmetric localization patterns seen occasionally at the 2-cell stage (B) and consistently in the 4-cell stage.
(D–F) Histological sections through animal hemisphere of 4-cell embryos confirm that the mRNA localization is preferentially localized within right ventral blastomeres (red arrowheads) and depleted from the left ventral blastomere (white arrowheads), but is symmetric in the smaller dorsal blastomeres. Dorsal is oriented to the top in (C–F).
(G) Dorsal view of an 8-cell embryo showing LR symmetrical expression in the dorsal animal blastomeres and the narrow band of mRNA on the animal side of the dorsovegetal blastomeres (arrowhead).
(H) After MBT (stage 8), H^+/K^+-ATPase α mRNA is expressed symmetrically throughout the animal cap, as visualized in transverse histological section.
(I) H^+/K^+-ATPase α mRNA is localized in neural tissues and posterior gut of tailbud stage (stage 32) embryos.
(J and K) HH stage 3^+ chick embryos showing symmetrical expression of H^+/K^+-ATPase α and β subunit mRNAs. The mRNAs remain symmetrically expressed in the ridges of the primitive streak at all stages examined (HH stages 2^+ to 4^-).

Misexpression of H^+/K^+-ATPase Subunits with Kir4.1 Perturbs LR Asymmetry

To confirm the pharmacologic loss-of-function data, we injected synthetic mRNA encoding H^+/K^+-ATPase subunits into 1-cell stage *Xenopus* embryos to determine if perturbing the endogenous pattern would induce heterotaxia. As shown in Figure 5, injection of α or β subunits alone yielded a negligible effect on the incidence of heterotaxia, while both together increased the incidence to a modest but statistically significant level. In various epithelia, outward K^+ current (through channels such as Kir4.1 in gastric epithelia) function together with the H^+/K^+-ATPase to hyperpolarize membrane potentials (Fujita et al., 2002; Ikuma et al., 1998; Meneton et al., 1999). Whereas the Kir4.1 misexpression with either subunit singly did not cause heterotaxia, a robust response was observed when both α and β H^+/K^+-ATPase subunits were injected together with Kir4.1. Interestingly, heterotaxia was observed only when embryos were injected before completion of the first cell division that gives rise to two blastomeres. Later injections did not cause heterotaxia; thus, it was not possible to use misexpression to probe the biological importance of the right-sided localization of endogenous transcripts, presumably because the time lag to synthesize proteins from the injected mRNAs is too long to override LR asymmetry determination by endogenous H^+/K^+-ATPase function.

Consistent LR Asymmetries in Cell Membrane Voltage Potential Exist across the Early Primitive Streak in Chick Embryos

In chick embryos, H^+/K^+-ATPase α (Figure 4J) and β (Figure 4K) subunit mRNAs are first detected by HH stage 2^+ to 4^- in a symmetric pattern along both sides of primitive streak, consistent with sensitivity to H^+/K^+-ATPase inhibitors prior to asymmetric gene expression at stage 5 (Figure 3). In light of the strikingly asymmetric localization of H^+/K^+-ATPase α mRNA in *Xenopus*, the symmetric expression in the chick led us to ask if the function of the ATPase might be asymmetrically constrained. The chick embryo is a flat disk making it amenable to microscopic imaging of membrane voltage potentials by fluorescent dye technology. *Xenopus*, in contrast, is spherical and exhibits high background autofluorescence. Embryos were incubated with $DiBAC_4(3)$,

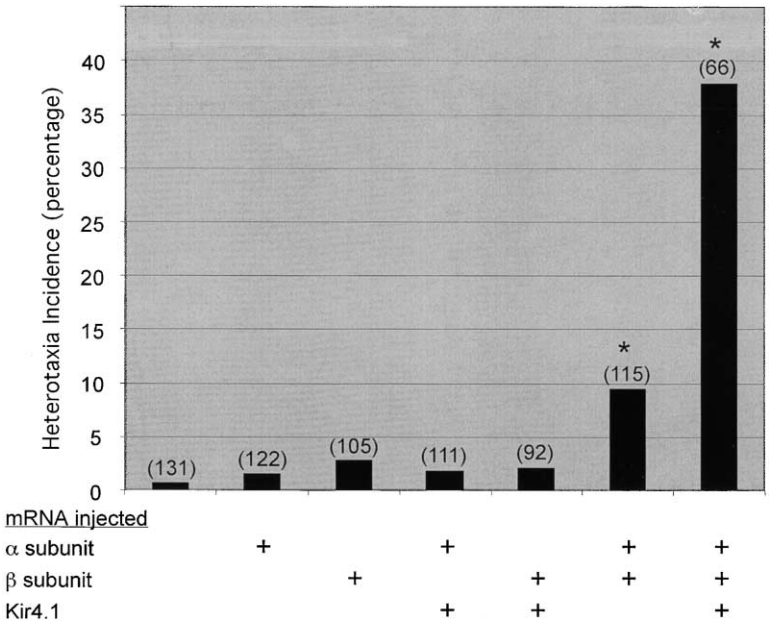

Figure 5. Heterotaxia Following Misexpression of H^+/K^+-ATPase α and β Subunits and the Kir4.1 Potassium Channel

Xenopus embryos were injected at the 1-cell stage with mRNAs encoding H^+/K^+-ATPase α and β subunits and Kir4.1. The incidence of heterotaxia (percentage of heterotaxic embryos) was scored as in Figure 1. α and β subunits expressed together, but not alone, induced statistically significant (*, $p < 0.001$) incidence of heterotaxia. Kir4.1 further increased the incidence of heterotaxic embryos when coexpressed with both H^+/K^+-ATPase subunits.

which accumulates in a voltage dependent manner, and the fluorescence intensity was measured (see Experimental Procedures). In stage 1–2 embryos, we observed a homogenous distribution of the fluorescence in the embryo, indicating an equivalent resting membrane potential in all cells of the blastoderm (Figure 6A). When primitive streak formation has progressed (HH stage 3), an increase in fluorescence was seen to the left of the streak, representing less negative membrane potentials, i.e., depolarized relative to cells to the right of the streak and throughout the epiblast (Figure 6B). At HH stage 3, the domain of depolarized cells extended from the base of the streak to Hensen's node. The area of depolarized cells was concentrated to the left side of Hensen's node in HH stage 4^- embryos (Figure 6C) and gradually diminished by HH stage 4^+ (Figure 6D). The gradual increase and later decrease in left-sided fluorescence is visible in linescans of these embryos (Figures 6E–6H). Mean fluorescence intensities were calculated from linescans and the magnitude of left-sided fluorescence intensity over that on the right side of the streak was 19.1% at HH stage 3, rising to 21.2% at HH stage 4^-, and diminishing to 6.8% at HH stage 4^+ (Supplemental Table S3 available at http://www.cell.com/cgi/content/full/111/1/77/DC1). No differences could be seen at HH stages 1–2. A 1% difference in $DiBAC_4(3)$ fluorescence corresponds to a membrane potential difference of about 1 mV (Brauner et al., 1984); thus, the magnitude of the endogenous left-sided depolarization is approximately 10–20 mV.

The Streak LR Voltage Asymmetry Is Due to H^+/K^+-ATPase Function

We then asked whether the asymmetry in membrane voltage potential is due to the activity of the H^+/K^+-ATPase pump. HH stage 3–4 embryos were imaged as before. The characteristic left-sided elevated fluorescence intensity was observed (Figure 6I) at which time either omeprazole or $BaCl_2$ was added to the culture. After 10–15 min of incubation, both the left and right sides or the primitive streak showed domains of elevated fluorescence (4/4 embryos treated with $BaCl_2$; 3/3 embryos treated with omeprazole; Figures 6J and 6K). Linescans made perpendicular to the streak show the corresponding fluorescence intensities following treatment (Figures 6L–6N). Thus, the inhibitor results suggest that H^+/K^+-ATPase activity normally prevents membrane depolarization in the domain on the right side of the streak. These data suggest a model in which H^+/K^+-ATPase function is required to the right of the midline in both *Xenopus* and chick embryos and that asymmetry is achieved in *Xenopus* at the level of mRNA localization while in the chick it is controlled downstream of mRNA expression.

Discussion

We describe the first results of a pharmacological screen using laterality of three visceral organs in *Xenopus* embryos as an endpoint. The specificity of many of the hits suggested the involvement of K^+ and H^+ flux and we report the specific involvement of H^+/K^+ ATPase function in both *Xenopus* and chick embryos.

A Role for H^+/K^+-ATPase in LR Patterning

The distribution of organ reversals that arose from inhibitors of K^+ channels and H^+/K^+-ATPases indicated that the defect elicited is heterotaxia, rather than isomerism or situs inversus. Thus, the individual organs in the preponderance of treated embryos developed asymmetrically, but with frequent reversals and discordance (Figure 1 and Supplemental Table S1 available at http://www.cell.com/cgi/content/full/111/1/77/DC1). Heterotaxia, however, is a complex phenotype and three points should be noted in interpreting the absolute incidences arising from each trial. Firstly, drug doses were sufficiently low to avoid other development defects that might indirectly affect laterality. Perturbation in dor-

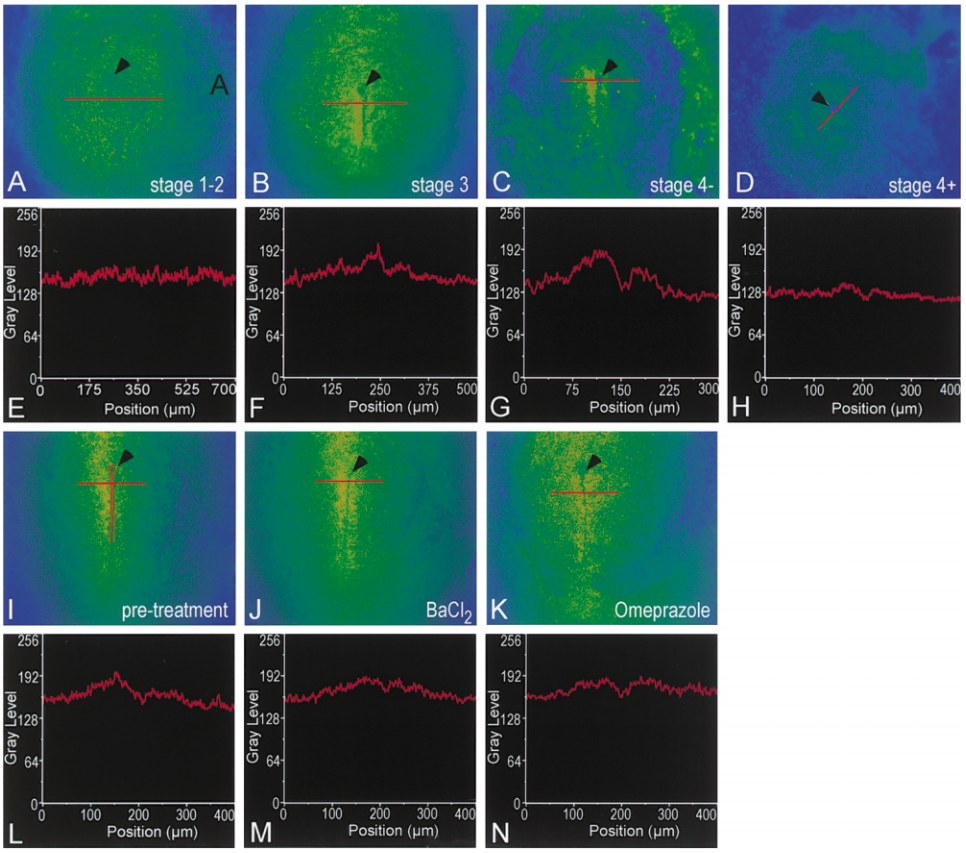

Figure 6. LR Asymmetries of Membrane Potential Patterns in the Primitive Streak Area Are Modulated by $BaCl_2$ or Omeprazole

(A–D) A transient domain of depolarization to the left side of the primitive streak in chick embryos visualized with the potentiometric fluorescent probe $DiBAC_4(3)$. The blue to green to red pseudo-color scale represents increasing fluorescence intensities reflecting increased accumulation of the anionic dye in intracellular membranes. Increased fluorescence corresponds to a less negative membrane potential (i.e., depolarized).

(E–H) Linescans of the embryos made perpendicular to the streak (red lines in A-D) show the increased left sided fluorescence. Supplemental Table S3, available at http://www.cell.com/cgi/content/full/111/1/77/DC1, summarizes the mean LR differences from all embryos tested.

(I–K) Typical LR asymmetric pattern of depolarization is seen prior to exposure (I). The streak is outlined in (I). A relative increase in right-sided fluorescence is seen in the same embryo as in (I) after exposure to $BaCl_2$ (J). Similar increase in right-sided fluorescence after omeprazole exposure (K). Arrowheads indicate Hensen's node.

(L–N) Linescans of the embryos (made along the red lines in I–K).

soanterior development, for instance, is commonly associated with LR defects (Danos and Yost, 1995). In our experiments, higher doses of NPPB, veratridine, or ouabain caused AP/DV patterning defects and heterotaxia in *Xenopus*. Secondly, although the maximum incidence of heterotaxia observed from the *complete* randomization of three independent organs would reach a theoretical maximum of 87.5%, laterality of certain organs such as gallbladder and gut are not entirely independent of one another (Casey and Hackett, 2000). Thirdly, a heterotaxic phenotype suggests that the initial biasing mechanism that orients LR axis in the embryo is either nonfunctional or uncoupled from organ morphogenesis, a conclusion supported by the loss of sided expression of all normally asymmetrically expressed genes examined (Figures 2, 3, and Supplemental Table S2 available at above website). In addition, SCH28080 gave identical results to omeprazole and lansoprazole, in support of specificity. Finally, omeprazole and lansoprazole are activated by acid and lower doses than described here were found to induce heterotaxia when the drugs were preincubated at pH 5.0 followed by neutralization (not shown), consistent with their pharmacology on gastric H^+/K^+-ATPases. Thus, we conclude that H^+ and K^+ flux, in particular as dependent on H^+/K^+-ATPase, is crucial for LR patterning upstream of the characterized cascades of asymmetric gene expression.

Laterality defects have not been reported in transgenic mice null for certain H^+/K^+-ATPase genes (Meneton et al., 1998; Spicer et al., 2000). Several explanations could account for the apparent discrepancy between the knockout phenotypes and our data. At least two isoforms of the H^+/K^+-ATPase are known to exist and it is plausible that compensatory or redundant function in the early embryo masks a laterality defect. Pharmacological studies, as we have done here, can be informative because the relatively broad specificity of inhibitors within the H^+/K^+-ATPase class allows targeting of multiple pump isoforms. To our knowledge, laterality defects have not been reported in mammalian teratogenicity studies of H^+/K^+-ATPase inhibitors, but this does not

seem to have been specifically examined. Thus, it will be of interest to analyze phenotypes arising from combinatorial deletions of genes encoding H^+/K^+-ATPase isoforms or from drug treatment in the mouse. In the absence of such data, it is not possible to predict whether or not LR asymmetry determination in the mouse involves H^+/K^+-ATPases or another system of pumps and channels. Pennekamp et al. (2002) provided evidence for the latter by observing heterotaxia and perturbations in asymmetric gene expression in a mouse with a targeted mutation in the polycystic kidney disease (PCKD) channel. Interestingly, at least one ion pump gene (encoding the sodium-calcium exchanger NCX-1) is expressed asymmetrically in Hensen's node of later stage chick embryos (Linask et al., 2001).

Localization of H^+/K^+-ATPase mRNA in *Xenopus*

Unexpectedly, H^+/K^+-ATPase α mRNA in *Xenopus* is asymmetrically localized by the 4-cell stage (Figures 4B–4F). This finding places a very early limit on when the initial biasing mechanism operates in the embryo. The amphibian egg is radially symmetrical and the point of sperm entry determines the dorsoventral and anteroposterior body axes of the embryo (Elinson, 1975; Gerhart et al., 1981; Scharf and Gerhart, 1980). LR asymmetry, therefore, is thought to be determined after fertilization. Our finding of consistently asymmetric mRNA in the 4-cell stage embryo suggests that the LR axis is oriented by about 2 hr of development in *Xenopus*. It is usually argued that LR asymmetry is determined later during cleavage or gastrula stages in vertebrates. In mice, for instance, the earliest known manifestation of LR asymmetry is the vortical rotation of monocilia on the ventral surface of node cells and the resultant fluid flow has been proposed to initiate asymmetry determination (Nonaka et al., 2002, 1998; Takeda et al., 1999). In the chick, the AP axis is first manifest by the location of Kohler's sickle and primitive streak in the blastoderm, which contains thousands of cells at this time. Whether LR asymmetry follows from this point, or if both LR and AP are patterned earlier in the chick remain uncertain. There are reports, however, of consistent LR differences in as early as the 2-cell stage in amphibians. These are manifest in the organ situs of embryos derived from separated left and right blastomeres (Spemann, 1938) and in the number of mitochondria that are found in each of the first 2 blastomeres in frog (Marinos, 1986). Indeed, Brown and Wolpert (1990) presented a prescient model of asymmetry determination in amphibians in which LR asymmetry determination was linked directly to the process of cortical rotation that establishes the AP and DV axes.

Localization of H^+/K^+-ATPase α mRNA in *Xenopus* precedes the known activation of the embryonic genome at the MBT (stage 8) when the embryo has roughly 1000 cells. Localization might involve selective mRNA degradation or cytoplasmic transport prior to complete separation of the cleaving blastomeres. Selective degradation is thought to localize *Drosophila* mRNAs such as *nanos* in the posterior polar plasm (Bashirullah et al., 1999) and linkage to motor proteins mediates the transport of mRNAs such as *bicoid* and *oskar* in *Drosophila* (Micklem et al., 2000; Schnorrer et al., 2000; Wilhelm et al., 2000) and *Ash1* in yeast (Beach et al., 2000; Munchow et al., 1999; Takizawa and Vale, 2000). Axonemal dynein (Supp et al., 1997) and kinesins (Takeda et al., 1999) have been demonstrated genetically to be involved in LR asymmetry in the mouse where they are thought to drive monociliary movement at the node. Our data, however, hint at novel functions for cytoplasmic motors in the determination of LR asymmetry.

Models of Ion Flux in LR Patterning

The H^+/K^+ exchanger works together with K^+ channels (Ikuma et al., 1998). The intracellular accumulation of K^+ ions is an active process mediated by a class of ATPases (P-type) that convert energy from the ATP/ADP ratio into an electrochemical K^+ gradient. Such ATPases exchange K^+ ions reciprocally with either Na^+ or H^+ ions, as for the H^+/K^+-ATPase implicated here in LR asymmetry determination. The K^+ accumulated in living cells exits passively through a variety of K^+ channels. Thus, the net potassium current, I_K, associated with H^+/K^+-ATPase function leads to a more negative (i.e., more polarized) membrane potential (Meneton et al., 1999). Our measurements using $DiBAC_4(3)$ indicate that a domain of depolarization exists on the left side of the primitive streak in untreated HH stage 3 to 4 chick embryos (Figure 6, Supplemental Table S3 available at http://www.cell.com/cgi/content/full/111/1/77/DC1). Treatment with the H^+/K^+-ATPase inhibitor omeprazole or with $BaCl_2$ leads to bilateral domains (Figure 6), indicating that the H^+/K^+-ATPase and I_K normally functions to maintain the more negative membrane potential on the right side of the streak (Figure 7A). These data, together with the early right-sided localization of H^+/K^+-ATPase mRNA in *Xenopus* and the observation that drugs affecting K^+ flux cause heterotaxia and perturb sided gene expression, implicate H^+/K^+-ATPase function as a very early step in LR asymmetry determination.

How might H^+/K^+-ATPase function regulate asymmetric gene expression? A simple model is that H^+/K^+-ATPase function directly regulates synthesis or secretion of a diffusible determinant that then initiates the known cascades of asymmetrically expressed genes (Figure 7B). Another possibility (Figure 7C) is that the H^+/K^+-ATPase-dependent asymmetry in membrane voltage in the left and right sides of the embryo might influence intracellular communication through gap junctions. Although the endogenous pattern of gap junction communication (GJC) is essential for LR asymmetry determination in both chicks and *Xenopus* (Levin and Mercola, 1998, 1999), GJC cannot be the initiating process, since an upstream mechanism must orient the direction that putative LR determinants pass through the channels. Electrophoresis of determinants has been proposed for endogenous electric fields (Cooper et al., 1989; Lange and Steele, 1978; Robinson and Messerli, 1996; Rose, 1970) and is known to operate in the transport of material into *Drosophila* oocytes from surrounding nurse cells (Diehl-Jones, 1993; Woodruff et al., 1988; Woodruff and Telfer, 1980). By analogy, a voltage difference, such as across the streak in the chick or ventral midline in *Xenopus*, might direct the intercellular propagation of low molecular weight, charged determinants through gap junctions. Net asymmetric accumula-

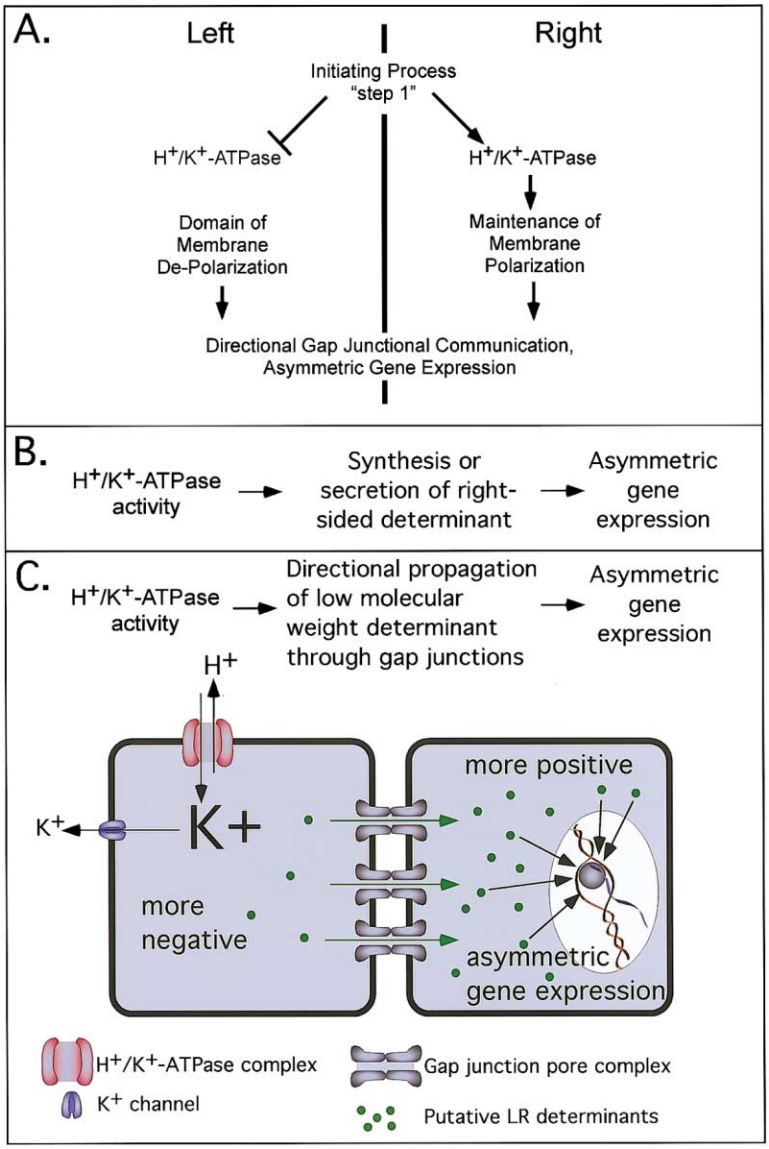

Figure 7. Models for Involvement of H^+/K^+-ATPase in Early LR Asymmetry

(A) Data presented here indicate that H^+/K^+-ATPase activity is localized to the right side of early *Xenopus* and chick embryos. An initiating mechanism to orient LR asymmetry has not been described experimentally in either chick or *Xenopus* but is envisaged to be responsible for the asymmetric H^+/K^+-ATPase activities, by localization of mRNA (*Xenopus*) or posttranslationally (chick), as described in the text.

(B) H^+/K^+-ATPase function might directly regulate the secretion of an early determinant of asymmetric gene expression.

(C) Alternatively, the H^+/K^+-ATPase might influence the propagation of unknown, low molecular weight LR determinants (green dots) between cells. Unidirectional propagation might rely simply on electrophoresis of charged determinants through open gap junction channels (depicted) or connexon gating (see text). The segregation of determinants triggers asymmetric expression of genes in multicellular fields.

tion or localization might then bias asymmetric gene expression. An alternate model is that H^+/K^+-ATPase activity might influence GJC via voltage and/or pH gating (Brink, 2000; Morley et al., 1997; White et al., 1994), which has been demonstrated in the frog embryo (Turin and Warner, 1980).

Regardless of how H^+/K^+-ATPase function and K^+ flux are coupled to gene expression, it is important to note that asymmetric H^+/K^+-ATPase function cannot be the initiating step of LR asymmetry determination, since some upstream factor must localize H^+/K^+-ATPase mRNA (as in *Xenopus*) or function (as in chick). One of the principal findings in this paper is that H^+/K^+-ATPase mRNA becomes localized in the 4-cell *Xenopus* embryo, thus restricting the timing of the initiating event to the first few hours of development. Brown and Wolpert (1990) proposed a conceptual model in which LR asymmetry is polarized when a chiral molecule becomes oriented with respect to the AP and DV axes. It is easiest to envision the chiral molecule as subcellular, while the middle phase of LR patterning features large-scale, multi-cellular fields of gene expression. Our models have the advantage of using asymmetries in K^+ and H^+ flux and GJC to leverage cell-based chirality into large-scale multi-cellular asymmetry.

Experimental Procedures

Xenopus Embryology

Xenopus embryos were dejellied in 2% cysteine 30′ after artificial fertilization and washed in 0.1×MMR. Batches of eggs from a single female were divided into several experimental and control groups. Each group was put into either 10 ml of 0.1×MMR (Marc's modified Ringer's solution) (controls) or 0.1×MMR containing drugs at the following doses: spermine, 395 μM; PCMB (p-chloromercuribenzoic acid), 277 μM; amantadine, 266 μM; IAA-94, 55 μM; NPPB (PAA), 3 μM; 9-AC (ACA), 68 μM; tetrodotoxin, 31 μM; veratridine, 0.2 μM; quinidine, 1.5 mM; lanthanum, 100 μM; amiodarone, 88 μM; barium chloride, 4 mM; Chromanol 293B, 100 μM; lansoprazole, 27 μM; omeprazole, 28 μM; SCH28080, 100 μM; amiloride, 2.2 mM; EIPA, 83 μM; ouabain, 10 μM; cariporide, 2.6 mM; and aurovertin, 400 μM. In all cases, levels of vehicle (DMSO for compounds which are

not water soluble) was $< 0.5\%$ (which permits normal LR development). Embryos were allowed to develop in the drug-containing medium until stage 16 (Nieuwkoop and Faber, 1967), at which point they were washed three times in 0.1×MMR and allowed to develop in 0.1×MMR + 0.1% gentamycin until stage 45.

Xenopus Injections

Capped, synthetic mRNA was transcribed in vitro (Ambion Message Machine) from linearized plasmid templates. mRNA was mixed with 50 ng of rhodamine-lysinated dextran (10,000 MW, Molecular Probes) and 320 pg of mRNA encoding β-galactosidase (as lineage labels) and injected into embryos within 30–45 min of fertilization. The approximate doses (per cell) were H^+/K^+-ATPase (*Xenopus* α, 100 pg) (*Bufo* β, 200 pg), mammalian Kir4.1/Bir10 (200 pg). H^+/K^+-ATPase cDNAs were obtained from Kaithi Geering (Institute of Pharmacology and Toxicology, Switzerland); and the Kir4.1/Bir10 cDNA was from John Adelman (Oregon Health Sciences University).

Chick Embryology

All experimental manipulations were performed on standard pathogen-free white leghorn chick embryos obtained from Charles River Laboratories (SPAFAS). Embryos were staged according to Hamburger and Hamilton (1992). Embryos were treated with inhibitors either by addition to filter culture or by injection directly into the albumin in ovo. Filter culture of control embryos does not alter asymmetric gene expression (Levin and Mercola, 1999). Generally, however, drug treatment in ovo yielded a lower incidence of asymmetric gene expression, presumably because of a lower local concentration after injection into the egg. In ovo treatment was used for examination of heart looping (Figure 1) and for some of the embryos examined for *Pitx2* and *car* expression (Supplemental Table S2B and S2C available at http://www.cell.com/cgi/content/full/111/1/77/DC1). For in ovo exposure, 0.5 ml of drug at the stated dose (in albumin) was injected directly into the albumin of each unincubated egg. The needle hole was covered with electrical tape and the egg incubated in a nonrotating 38°C incubator. For culture, embryos were explanted in Pannett-Compton medium under a dissecting microscope. The embryo was placed ventral side upward on a Costar 1 μm filter (catalog #110410) floating on top of medium consisting of 0.5 ml of Alpha-MEM medium (with or without drug) in 40 ml of thin albumin. Embryos were then cultured at 38°C until the required stage of development.

Scoring *Xenopus* Embryonic Situs

The phenotype of embryos was determined by scoring the situs of the heart, stomach, and gallbladder under a dissecting microscope using tricaine to immobilize the stage 45 embryos. Only embryos with normal dorsoanterior development (DAI = 5) and clear left-sided or right-sided organs were scored. Embryos with ambiguous (unscoreable) situs comprised less than 5% of each experiment. A heterotaxic embryo was considered to be one in which any of those three organs was reversed in its position. The incidences of organ situs were analyzed using the chi-square test with Pearson correction (for sample size).

In Situ Hybridization

Chick embryos were fixed in 4% paraformaldehyde at 4°C overnight (for cultured embryos, filters with embryos were transferred to 4% paraformaldehyde and the embryos were carefully detached). Frog embryos were fixed in MEMFA (Harland, 1991) at 4°C overnight. cDNA used to transcribe cRNA in situ hybridization probes were: *cShh* and *cNodal* (Levin et al., 1995), *cCerberus/caronte* (Zhu et al., 1999), *cPitx-2* (Logan et al., 1998), *cfgf8* (Boettger et al., 1999; Ohuchi et al., 2000), *cWnt8c* (Levin, 1998; Rodriguez-Esteban et al., 2001), *cH$^+$/K$^+$-ATPase* α (GenBank accession number AL588035, obtained from Frazer Murray), *cH$^+$/K$^+$-ATPase* β (Yu et al., 1994), and *XH$^+$/K$^+$-ATPase* α (Mathews et al., 1995). Histological sections were obtained by embedding embryos after in situ hybridization in JB4 according to manufacturer's directions (Polysciences).

Chick Membrane Potential Measurements

For the study of membrane potential patterns, the embryos were incubated in the fluorescent membrane potential sensitive probe bis-(1,3-dibutyrlbarbituric acid)thrimethine oxonol) [$DiBAC_4(3)$] (Molecular Probes Inc, Eugene, OR, USA; Epps et al., 1994). $DiBAC_4(3)$ is an anionic fluorescent molecule that is distributed into intracellular membranes depending on the electrical potential across the plasma membrane. The more depolarized, i.e., the less negative the membrane potential is, the more anionic probe is accumulated, giving an increased fluorescent signal from the cell. The experiments were performed in ovo. A round opening was cut in the egg after 8–18 hr of incubation at 38°C, and some of the thick albumen was removed by the use of a fire polished Pasteur pipette. A Plexiglas ring (diameter 1.5 cm) was placed on the yolk surrounding the embryo to minimize the amount of chemicals used. $DiBAC_4(3)$ was dissolved in 70% ethanol at 1 mg/ml and further diluted in deionized water to a final concentration of 100 μg/ml. Portions of 100 μl from these solutions were added to 900 μl of Panett-Compton buffer [pH 7.4], to give final dye concentrations of 10 μg/ml, and the embryos were incubated with the probe for 20–30 min at room temperature. The fluorescence measurements were made in an upright epifluorescent microscope (Zeiss Axiophot) with a 2.5× Neofluor lens (NA 0.075), and the images were sampled with a cooled CCD camera (Princeton Instruments Inc., NJ, USA). High potassium concentrations (50 mM) were used to test for dye efficacy and cell viability. This treatment depolarized the cells, as seen by an increase in the fluorescence. In the blocking experiments, 1 mg/ml $BaCl_2$ or 100 μg/ml omeprazole (Sigma Chemical Co. St. Louis, MO, USA) were added after the 20–30 min probe incubation or together with the probe at the start of the incubation. The data were analyzed with a MetaMorph image analysis program (Universal Imaging Corp., PA, USA). The fluorescence (F) was calculated from a linescans of the left sided ($F_L = F_{left}/F_{min}$) and right-sided ($F_R = F_{right}/F_{min}$) fluorescences, respectively. F_{min} represents the lowest fluorescence intensity value in transverse linescans over the whole embryo; F_L and F_R were peak intensity values. The difference between left- and right-sided fluorescence is $dF = F_L - F_R$, and the change in fluorescence presented as $dF/F_L \times 100$. The values obtained were reproducible for different embryos (Supplemental Table S3 available at http://www.cell.com/cgi/content/full/111/1/77/DC1).

Acknowledgments

This paper is dedicated to Lionel Jaffe, whose research inspired these studies. We thank Adam Crook, Debra Sorocco, and Shing-Ming Cheng for their expert technical assistance. We acknowledge AstraZeneca, Takeda Chemical Industries, and Schering-Plough Co. for their generous gifts of omeprazole, lansoprazole, and SCH28080, respectively. Once commercially available, these drugs were purchased from Sigma. We also thank Gary Yellen, Frederic Jaisser, and George Sachs for many helpful discussions, and Ralph Kent for advice on statistical analysis. We are grateful for chick H^+/K^+-ATPase α cDNA from Frazer Murray; the chick H^+/K^+-ATPase β cDNA from K. Takeyasu; the *Xenopus* H^+/K^+-ATPase β and *Bufo* α cDNAs from Kaithi Geering; and the Kir4.1/Bir10 cDNA from John Adelman. M.L. gratefully acknowledges a Helen Hay Whitney Foundation postdoctoral fellowship and grants from the American Cancer Society (RSG-02-046-01), Chestnut Hill Charitable Foundation, and the American Heart Association (Beginning Grant in Aid, 0160263T). K.R.R. gratefully acknowledges support from the NSF (008517-IBN) and M.M. gratefully acknowledges grants from the NIH (RO1 HL63271) and American Heart Association (Established Investigator Award, 9740005N).

Received: December 12, 2001
Revised: August 15, 2002

References

Altizer, A., Moriarty, L., Bell, S., Schreiner, C., Scott, W., and Borgens, R. (2001). Endogenous electric current is associated with normal development of the vertebrate limb. Dev. Dyn. *221*, 391–401.

Bashirullah, A., Halsell, S.R., Cooperstock, R.L., Kloc, M., Karaiskakis, A., Fisher, W.W., Fu, W., Hamilton, J.K., Etkin, L.D., and Lipshitz, H.D. (1999). Joint action of two RNA degradation pathways

controls the timing of maternal transcript elimination at the midblastula transition in *Drosophila melanogaster*. EMBO J. *18*, 2610–2620.

Beach, D.L., Thibodeaux, J., Maddox, P., Yeh, E., and Bloom, K. (2000). The role of the proteins Kar9 and Myo2 in orienting the mitotic spindle of budding yeast. Curr. Biol. *10*, 1497–1506.

Boettger, T., Wittler, L., and Kessel, M. (1999). FGF8 functions in the specification of the right body side of the chick. Curr. Biol. *9*, 277–280.

Borgens, R., and Shi, R. (1995). Uncoupling histogenesis from morphogenesis in the vertebrate embryo by collapse of the transneural tube potential. Dev. Dyn. *203*, 456–467.

Brauner, T., Hulser, D., and Strasser, R. (1984). Comparative measurements of membrane potentials with microelectrodes and voltage-sensitive dyes. Biochim. Biophys. Acta *771*, 208–216.

Brink, P. (2000). Gap junction voltage dependence: a clear picture emerges. J. Gen. Physiol. *116*, 11–12.

Brown, N., and Wolpert, L. (1990). The development of handedness in left/right asymmetry. Development *109*, 1–9.

Burdine, R., and Schier, A. (2000). Conserved and divergent mechanisms in left-right axis formation. Genes Dev. *14*, 763–776.

Capdevila, J., Vogan, K., Tabin, C., and Belmonte, J.I. (2000). Mechanisms of left-right determination in vertebrates. Cell *101*, 9–21.

Casey, B. (1998). Two rights make a wrong: human left-right malformations. Hum. Mol. Genet. *7*, 1565–1571.

Casey, B., and Hackett, B.P. (2000). Left-right axis malformations in man and mouse. Curr. Opin. Genet. Dev. *10*, 257–261.

Cooper, M.S., Miller, J.P., and Fraser, S.E. (1989). Electrophoretic repatterning of charged cytoplasmic molecules within tissues coupled by gap junctions by externally applied electric fields. Dev. Biol. *132*, 179–188.

Croyle, M.L., Woo, A.L., and Lingrel, J.B. (1997). Extensive random mutagenesis analysis of the Na+/K+-ATPase alpha subunit identifies known and previously unidentified amino acid residues that alter ouabain sensitivity—implications for ouabain binding. Eur. J. Biochem. *248*, 488–495.

Danos, M., and Yost, H. (1995). Linkage of cardiac left-right asymmetry and dorsal-anterior development in *Xenopus*. Development *121*, 1467–1474.

Diehl-Jones, W. (1993). Ionic basis of bioelectric currents during oogenesis in an insect. Dev. Biol. *158*, 301–316.

Elinson, R.P. (1975). Site of sperm entry and a cortical contraction associated with egg activation in the frog Rana pipiens. Dev. Biol. *47*, 257–268.

Epps, D., Wolfe, M., and Groppi, V. (1994). Characterization of the steady-state and dynamic fluorescence properties of the potential-sensitive dye bis-(1,3-dibutylbarbituric acid)trimethine oxonol (Dibac4(3)) in model systems and cells. Chem. Phys. Lipids *69*, 137–150.

Fujita, A., Horio, Y., Higashi, K., Mouri, T., Hata, F., Takeguchi, N., and Kurachi, Y. (2002). Specific localization of an inwardly rectifying K+ channel, Kir4.1, at the apical membrane of rat gastric parietal cells; its possible involvement in K+ recycling for the H+-K+ pump. J. Physiol. *540*, 85–92.

Gerhart, J., Ubbels, G., Black, S., Hara, K., and Kirschner, M. (1981). A reinvestigation of the role of the grey crescent in axis formation in *Xenopus laevis*. Nature *292*, 511–516.

Gottardi, C.J., and Caplan, M.J. (1993a). An ion-transporting ATPase encodes multiple apical localization signals. J. Cell Biol. *121*, 283–293.

Gottardi, C.J., and Caplan, M.J. (1993b). Molecular requirements for the cell-surface expression of multisubunit ion-transporting ATPases. Identification of protein domains that participate in Na,K-ATPase and H,K-ATPase subunit assembly. J. Biol. Chem. *268*, 14342–14347.

Hamburger, V., and Hamilton, H. (1992). A series of normal stages in the development of the chick embryo. Dev. Dyn. *195*, 231–272.

Harland, R.M. (1991). In situ hybridization: an improved whole mount method for *Xenopus* embryos. In *Xenopus laevis*: Practical Uses in Cell and Molecular Biology, B.K. Kay, and H.B. Peng, eds. (San Diego: Academic Press), pp. 685–695.

Harris, C., and Fliegel, L. (1999). Amiloride and the Na(+)/H(+) exchanger protein: mechanism and significance of inhibition of the Na(+)/H(+) exchanger (review). Int. J. Mol. Med. *3*, 315–321.

Hotary, K., and Robinson, K. (1992). Evidence of a role for endogenous electric fields in chick embryo development. Development *114*, 985–996.

Hotary, K.B., and Robinson, K.R. (1994). Endogenous electrical currents and voltage gradients in *Xenopus* embryos and the consequences of their disruption. Dev. Biol. *166*, 789–800.

Hyatt, B., and Yost, H. (1998). The left-right coordinator: the role of Vg1 in organizing left-right axis. Cell *93*, 37–46.

Ikuma, M., Binder, H., and Geibel, J. (1998). Role of apical H-K exchange and basolateral K channel in the regulation of intracellular pH in rat distal colon crypt cells. J. Membr. Biol. *166*, 205–212.

Jaffe, L. (1981). The role of ionic currents in establishing developmental pattern. Philos. Trans. R. Soc. Lond. B. Biol. Sci. *295*, 553–566.

Jiang, Y., and MacKinnon, R. (2000). The barium site in a potassium channel by x-ray crystallography. J. Gen. Physiol. *115*, 269–272.

Lange, C.S., and Steele, V.E. (1978). The mechanism of anterior-posterior polarity control in planarians. Differentiation *11*, 1–12.

Levin, M. (1998). Left-right asymmetry and the chick embryo. Semin. Cell Dev. Biol. *9*, 67–76.

Levin, M., and Mercola, M. (1998). Gap junctions are involved in the early generation of left right asymmetry. Dev. Biol. *203*, 90–105.

Levin, M., and Mercola, M. (1999). Gap junction-mediated transfer of left-right patterning signals in the early chick blastoderm is upstream of Shh asymmetry in the node. Development *126*, 4703–4714.

Levin, M., Johnson, R., Stern, C., Kuehn, M., and Tabin, C. (1995). A molecular pathway determining left-right asymmetry in chick embryogenesis. Cell *82*, 803–814.

Linask, K., Han, M., Artman, M., and Ludwig, C. (2001). Sodium-calcium exchanger (NCX-1) and calcium modulation: NCX protein expression patterns and regulation of early heart development. Dev. Dyn. *221*, 249–264.

Logan, M., Pagan-Westphal, S., Smith, D., Paganessi, L., and Tabin, C. (1998). The transcription factor Pitx2 mediates situs-specific morphogenesis in response to left-right asymmetric signals. Cell *94*, 307–317.

Lohr, J., Danos, M., and Yost, H. (1997). Left-right asymmetry of a *nodal*-related gene is regulated by dorsoanterior midline structures during *Xenopus* development. Development *124*, 1465–1472.

Marinos, E. (1986). Observations on the mitochondrial distribution in normal, rotated and cold-treated 2-cell stage embryos of *Xenopus laevis*. Cell Differ. *18*, 163–171.

Mathews, P.M., Claeys, D., Jaisser, F., Geering, K., Horisberger, J.D., Kraehenbuhl, J.P., and Rossier, B.C. (1995). Primary structure and functional expression of the mouse and frog alpha-subunit of the gastric H(+)-K(+)-ATPase. Am. J. Physiol. *268*, C1207–1214.

Mathur, S., and Karmazyn, M. (1997). Interaction between anesthetics and the sodium-hydrogen exchange inhibitor HOE 642 (cariporide) in ischemic and reperfused rat hearts. Anesthesiology *87*, 1460–1469.

Meneton, P., Schultheis, P.J., Greeb, J., Nieman, M.L., Liu, L.H., Clarke, L.L., Duffy, J.J., Doetschman, T., Lorenz, J.N., and Shull, G.E. (1998). Increased sensitivity to K+ deprivation in colonic H,K-ATPase-deficient mice. J. Clin. Invest. *101*, 536–542.

Meneton, P., Lesage, F., and Barhanin, J. (1999). Potassium ATPases, channels, and transporters: an overview. Semin. Nephrol. *19*, 438–457.

Mercola, M., and Levin, M. (2001). Left-right asymmetry determination in vertebrates. Annu. Rev. Cell Dev. Biol. *17*, 779–805.

Micklem, D.R., Adams, J., Grunert, S., and St Johnston, D. (2000). Distinct roles of two conserved Staufen domains in oskar mRNA localization and translation. EMBO J. *19*, 1366–1377.

Mizunashi, K., Furukawa, Y., Katano, K., and Abe, K. (1993). Effect

of omeprazole, an inhibitor of H+,K(+)-ATPase, on bone resorption in humans. Calcif. Tissue Int. *53*, 21–25.

Morley, G.E., Ek-Vitorin, J.F., Taffet, S.M., and Delmar, M. (1997). Structure of connexin43 and its regulation by pHi. J. Cardiovasc. Electrophysiol. *8*, 939–951.

Munchow, S., Sauter, C., and Jansen, R.P. (1999). Association of the class V myosin Myo4p with a localised messenger RNA in budding yeast depends on She proteins. J. Cell Sci. *112*, 1511–1518.

Munson, K.B., Lambrecht, N., and Sachs, G. (2000). Effects of mutations in M4 of the gastric H+,K+-ATPase on inhibition kinetics of SCH28080. Biochemistry *39*, 2997–3004.

Nieuwkoop, P.D., and Faber, J. (1967). Normal Table of *Xenopus laevis* (Daudin), Second Edition (Amsterdam: North-Holland Publishing Company).

Nonaka, S., Tanaka, Y., Okada, Y., Takeda, S., Harada, A., Kanai, Y., Kido, M., and Hirokawa, N. (1998). Randomization of left-right asymmetry due to loss of nodal cilia generating leftward flow of extraembryonic fluid in mice lacking KIF3B motor protein. Cell *95*, 829–837.

Nonaka, S., Shiratori, H., Saijoh, Y., and Hamada, H. (2002). Determination of left-right patterning of the mouse embryo by artificial nodal flow. Nature *418*, 96–99.

Ohuchi, H., Kimura, S., Watamoto, M., and Itoh, N. (2000). Involvement of fibroblast growth factor (FGF)18–FGF8 signaling in specification of left-right asymmetry and brain and limb development of the chick embryo. Mech. Dev. *95*, 55–66.

Pagan-Westphal, S., and Tabin, C. (1998). The transfer of left-right positional information during chick embryogenesis. Cell *93*, 25–35.

Pennekamp, P., Karcher, C., Fischer, A., Schweickert, A., Skryabin, B., Horst, J., Blum, M., and Dworniczak, B. (2002). The ion channel polycystin-2 is required for left-right axis determination in mice. Curr. Biol. *12*, 938–943.

Pizzonia, J.H., Ransom, B.R., and Pappas, C.A. (1996). Characterization of Na+/H+ exchange activity in cultured rat hippocampal astrocytes. J. Neurosci. Res. *44*, 191–198.

Psychoyos, D., and Stern, C. (1996). Restoration of the organizer after radical ablation of Hensen's node and the anterior primitive streak in the chick embryo. Development *122*, 3263–3273.

Robinson, K., and Messerli, M. (1996). Electric embryos: the embryonic epithelium as a generator of developmental information. In Nerve Growth and Guidance, C. McCaig, ed. (Portland: Portland Press).

Rodriguez-Esteban, C., Capdevila, J., Kawakami, Y., and Izpisua Belmonte, J.C. (2001). Wnt signaling and PKA control Nodal expression and left-right determination in the chick embryo. Dev. Suppl. *128*, 3189–3195.

Rose, S.M. (1970). Differentiation during regeneration caused by migration of repressors in bioelectric fields. Am. Zool. *10*, 91–99.

Sachs, G., Shin, J.M., Briving, C., Wallmark, B., and Hersey, S. (1995). The pharmacology of the gastric acid pump: the H+,K+ ATPase. Annu. Rev. Pharmacol. Toxicol. *35*, 277–305.

Sanders, S.W., Tolman, K.G., Greski, P.A., Jennings, D.E., Hoyos, P.A., and Page, J.G. (1992). The effects of lansoprazole, a new H+,K(+)-ATPase inhibitor, on gastric pH and serum gastrin. Aliment. Pharmacol. Ther. *6*, 359–372.

Scharf, S.R., and Gerhart, J.C. (1980). Determination of the dorsal-ventral axis in eggs of *Xenopus laevis*: complete rescue of uv-impaired eggs by oblique orientation before first cleavage. Dev. Biol. *79*, 181–198.

Schnorrer, F., Bohmann, K., and Nusslein-Volhard, C. (2000). The molecular motor dynein is involved in targeting swallow and bicoid RNA to the anterior pole of *Drosophila* oocytes. Nat. Cell Biol. *2*, 185–190.

Shi, R., and Borgens, R. (1994). Embryonic neuroepithelial sodium transport, the resulting physiological potential, and cranial development. Dev. Biol. *165*, 105–116.

Shi, R., and Borgens, R.B. (1995). Three-dimensional gradients of voltage during development of the nervous system as invisible coordinates for the establishment of embryonic pattern. Dev. Dyn. *202*, 101–114.

Spemann, H. (1938). Embryonic Development and Induction (New Haven, CT: Yale University Press).

Spicer, Z., Miller, M.L., Andringa, A., Riddle, T.M., Duffy, J.J., Doetschman, T., and Shull, G.E. (2000). Stomachs of mice lacking the gastric H,K-ATPase alpha-subunit have achlorhydria, abnormal parietal cells, and ciliated metaplasia. J. Biol. Chem. *275*, 21555–21565.

Supp, D., Witte, D., Potter, S., and Brueckner, M. (1997). Mutation of an axonemal dynein affects left-right asymmetry in inversus viscerum mice. Nature *389*, 963–966.

Supp, D., Brueckner, M., Kuehn, M., Witte, D., Lowe, L., McGrath, J., Cirrakes, J., and Potter, S. (1999). Targeted deletion of the ATP binding domain of left-right dynein confirms its role in specifying development of left-right asymmetries. Development *126*, 5495–5504.

Takeda, S., Yonekawa, Y., Tanaka, Y., Nonaka, Y.O.S., and Hirokawa, N. (1999). Left-right asymmetry and kinesin superfamily protein KIF3A. J. Cell Biol. *145*, 825–836.

Takeda, S., Yamazaki, H., Seog, D., Kanai, Y., Terada, S., and Hirokawa, N. (2000). Kinesin superfamily protein 3 (KIF3) motor transports fodrin-associating vesicles important for neurite building. J. Cell Biol. *148*, 1255–1265.

Takizawa, P.A., and Vale, R.D. (2000). The myosin motor, Myo4p, binds Ash1 mRNA via the adapter protein, She3p. Proc. Natl. Acad. Sci. USA *97*, 5273–5278.

Turin, L., and Warner, A.E. (1980). Intracellular pH in early *Xenopus* embryos: its effect on current flow between blastomeres. J. Physiol. *300*, 489–504.

Waddington, C. (1937). The dependence of head curvature on the development of the heart in the chick embryo. J. Exp. Biol. *14*, 229–231.

Weber, J., and Senior, A.E. (1998). Effects of the inhibitors azide, dicyclohexylcarbodiimide, and aurovertin on nucleotide binding to the three F1-ATPase catalytic sites measured using specific tryptophan probes. J. Biol. Chem. *273*, 33210–33215.

White, T.W., Bruzzone, R., Goodenough, D.A., and Paul, D.L. (1994). Voltage gating of connexins. Nature *371*, 208–209.

Wilhelm, J.E., Mansfield, J., Hom-Booher, N., Wang, S., Turck, C.W., Hazelrigg, T., and Vale, R.D. (2000). Isolation of a ribonucleoprotein complex involved in mRNA localization in *Drosophila* oocytes. J. Cell Biol. *148*, 427–440.

Woodruff, R., and Telfer, W. (1980). Electrophoresis of proteins in intercellular bridges. Nature *286*, 84–86.

Woodruff, R., Kulp, J., and LaGaccia, E. (1988). Electrically mediated protein movement in *Drosophila* follicles. Roux's Archives of Dev. Biol. *197*, 231–238.

Yost, H.J. (2001). Establishment of left-right asymmetry. Int. Rev. Cytol. *203*, 357–381.

Yu, H., Ishii, T., Pearson, W.R., and Takeyasu, K. (1994). Primary structure of avian H+/K(+)-ATPase β-subunit. Biochim. Biophys. Acta *1190*, 189–192.

Yuan, S., and Schoenwolf, G. (1998). De novo induction of the organizer and formation of the primitive streak in an experimental model of notochord reconstitution in avian embryos. Development *125*, 201–213.

Zhu, L., Marvin, M., Gardiner, A., Lassar, A., Mercola, M., Stern, C., and Levin, M. (1999). Cerberus regulates left-right asymmetry of the embryonic head and heart. Curr. Biol. *9*, 931–938.